The synergistic catalyst-carbonates effect on the direct bituminous coal fuel cell performance

N. Kaklidis[1,2], R. Strandbakke[3], A. Arenillas[4], J.A. Menéndez[4], M. Konsolakis[5] and G.E. Marnellos[1,2,6*]

[1]*University of Western Macedonia, Department of Mechanical Engineering, Kozani, Greece*

[2]*University of Western Macedonia, Department of Environmental Engineering, Kozani, Greece*

[3]*Universitetet i Oslo, Department of Chemistry, Oslo, Norway*

[4]*Instituto Nacional del Carbón (INCAR-CSIC), Oviedo, Spain*

[5]*Technical University of Crete, School of Production Engineering and Management, Chania, Greece*

[6]*Chemical Process & Energy Resources Institute, Centre for Research & Technology Hellas, Thessaloniki, Greece*

To whom correspondence should be addressed

***Corresponding author. E-mail: gmarnellos@uowm.gr (G.E. Marnellos)**

ABSTRACT

The current work explores the feasibility to improve the performance of a Direct Carbon Fuel Cell (DCFC): CO_2 + bituminous coal|Co-CeO_2/YSZ/Ag|Air by infusing a gasification catalyst (Co/CeO_2) and/or Li-K carbonates mixture into the carbon fuel. The different fuel feedstock mixtures were characterized by various methods, involving chemical composition and proximate analysis, particle size distribution (PSD), X-ray diffraction (XRD), N_2 adsorption-desorption (BET method), thermogravimetric analysis (TGA) and scanning electron microscopy (SEM), to gain insight into the effect of catalyst and/or carbonates addition to fuel mixture physicochemical characteristics. An increase of the power output up to ca. 20 and 80% is achieved for carbon/catalyst and carbon/catalyst/carbonates mixtures, respectively, in comparison to bare carbon at 700 ^{o}C, demonstrating the pronounced effect of catalyst as well as its potential synergy with carbonates. It was also shown that the achieved maximum power density is directly associated with the CO formation rate, implying the importance of *in situ* formed CO on the electrochemical performance. The obtained findings are further discussed based also on the corresponding AC impedance spectroscopy studies, which revealed the beneficial effect of fuel feedstock additives (catalyst and/or carbonates) on ohmic and electrode polarization resistances. The present results clearly revealed the feasibility to improve the DCFC performance by concurrently infusing a gasification catalyst and carbonates mixture into fuel feedstock.

Keywords: DCFC, bituminous coal, Co/CeO_2 catalyst, carbonates, catalyst/carbonates synergy

1. INTRODUCTION

Coal is abundantly found around the globe accounted for ca. one third of the world energy consumption. More importantly, the currently proven reserves of coal are sufficient to meet more than 130 years of global production, approximately more than two times the reserves-to-production ratio for oil and natural gas [1]. However, conventional coal fired power plants, where coal is commonly converted to electricity, exhibit a low electrical efficiency, ranged in between 30 – 40%, accompanied by high pollutants emissions per produced MWh.

Direct Carbon Fuel Cells (DCFCs) are electrochemical energy devices, similar to conventional fuel cells, fueled, however, with solid feedstock instead of gaseous or liquid fuels [2-4]. In DCFCs the chemical energy contained in solid fuels is directly transformed to electricity at high efficiencies and low environmental impact [3-7]. Various solid fuels have been examined in DCFCs including, among others, various coal types, activated carbon, biomass, chars and organic wastes [8-17]. Compared to gaseous- and liquid-fed fuel cells, DCFCs are advantageous due to the high energy density of carbon, besides their high thermodynamic efficiency (ca. 100%) owing to the positive ΔS^o (2.9 J/K·mol) of carbon oxidation [18-23].

The reaction scheme in DCFCs is very complicated in comparison to hydrogen fed SOFCs [3-7, 20]. In particular, at the air exposed cathode oxygen is reduced to oxygen anions, O^{2-} (eq. 1), which then are transferred *via* the solid electrolyte into the anode three-phase boundary (TPB, the interphase between the solid electrolyte, electrode and gas/solid chemical species), where they react with solid carbon toward CO_2 (eq. 2):

$$O_2 + 4e^- \rightarrow 2O^{2-} \quad (1)$$

$$C + 2O^{2-} \rightarrow CO_2 + 4e^- \quad (2)$$

Alternatively, carbon could be electro-oxidized sequentially at first to CO (eq. 3) and then to CO_2 (eq. 4):

$$C + O^{2-} \rightarrow CO + 2e^- \quad (3)$$

$$CO + O^{2-} \rightarrow CO_2 + 2e^- \quad (4)$$

In the presence of molten carbonates in the solid feedstock (Hybrid Direct Carbon Fuel Cell, HDCFC), the carbon delivery to anode TPB is notably accelerated, partially bypassing the limitations derived from the solid-solid interactions in DCFCs [4, 5, 24]. Furthermore, in the presence of carbonates, several electrochemical reactions can concurrently take place in the anode chamber, leading to carbon consumption and power generation:

$$C + 2CO_3^{2-} \rightarrow 3CO_2 + 4e^- \quad (5)$$

$$C + CO_3^{2-} \rightarrow CO + CO_2 + 2e^- \quad (6)$$

$$2C + CO_3^{2-} \rightarrow 3CO + 2e^- \quad (7)$$

In addition, the CO_2 formed through the above reactions or fed as gasifying agent in fuel compartment can further interact with carbon to generate CO through the reverse Boudouard reaction (rBR; eq. 8):

$$C + CO_2 \rightarrow 2CO \quad (8)$$

This particular reaction is thermodynamically favored at temperatures higher than ca. 700 ^oC and its rate can be enhanced in the presence of a gasification catalyst in the fuel feedstock [2, 25-29]. Although the rBR is a chemical reaction not directly participating in the electrochemical reaction scheme, it can notably contribute to the DCFC performance [2, 13, 14, 21, 24, 25, 28]. More specifically, its gaseous product, CO, can be faster diffused and electro-oxidized at the anode TPB (eq. 4) as compared to solid carbon (eqs. 2 and 3), contributing to power generation.

Regarding the impact of fuel characteristics on the DCFC performance, it should be noted that coal is a conglomerate consisting of various organic and inorganic substances [13, 22]. For carbon fed DCFCs, the organic part of coal is the main reactant, while the corresponding inorganic content could degrade the DCFC performance and lifetime [11, 13, 15-17, 22, 30-35]. Therefore, the key parameters for a coal to exhibit a promising DCFC performance are its high carbon content and high reactivity of the carbonaceous matter towards favoring the electrochemical processes involving coal, and the low ash and sulfur content to minimize secondary degradation reactions [2, 9, 11-13, 27, 31, 36-42], characteristics which are presented in bituminous coal.

In this context, the current work targets to evaluate the electrochemical performance of a direct bituminous coal fuel cell: CO_2 + bituminous coal|Co-CeO_2/YSZ/Ag|Air in the absence and presence

of a gasification catalyst (Co/CeO_2) and/or carbonates (Li_2CO_3-K_2CO_3) into the fuel feed. To the best of our knowledge, the combined impact of catalyst and carbonates into the DCFC performance has not been reported previously. Interestingly, the results clearly reveal a synergistic catalyst-carbonates effect towards the development of highly efficient carbon fed fuel cells.

2. MATERIALS AND METHODS

2.1 Catalyst preparation

The 20 wt.% Co/CeO_2 employed both as anode electrode and catalyst infused to carbon feedstock mixture was synthesized using the wet impregnation method, as described in previous studies [2, 21, 35, 43].

2.2 Fuel feedstock preparation

In the present work bituminous coal (BC) was selected as fuel due to its unique intrinsic fuel characteristics including its high carbon content, high reactivity and fluidity of the coal when heated [2, 13, 27, 31, 36-42]. In addition, a bituminous coal of low mineral matter content and low sulphur content was employed, in order to minimize the undesirable reactions that could mask the DCFC electrochemical performance. The BC was appropriately milled and sieved so as to obtain particles lower than 50 microns, as verified by coulter analysis. The BC sample was next admixed with Co/CeO_2 and/or an eutectic mixture of 62 mol% Li_2CO_3 – 38 mol% K_2CO_3 (Sigma Aldrich) in order to obtain carbon/catalyst or carbon/catalyst/carbonates mixtures of a weight ratio of 4:2 or 4:2:1 respectively (800 mg carbon/400 mg Co/CeO_2/200 mg carbonate). For fuel feedstock preparation the bituminous coal was dissolved in *n*-hexane solvent and agitated in an ultrasonic device for 15 min before catalyst and/or carbonates mixture addition. The solution was then stirred at 70 ^oC for ca. 4 h until *n*-hexane evaporation [2, 13, 21, 25, 35, 43].

2.3 Materials characterization

The textural characteristics, in terms of BET surface area (S_{BET}) and total pore volume (V_p), of the fuel feedstock mixtures were obtained by N_2 adsorption-desorption isotherms at −196 °C. The structural and morphological characteristics of as-prepared fuel mixtures were assessed by means of X-ray Diffraction (XRD) and Scanning Electron Microscopy (SEM). The experimental setup and the procedure followed in the aforementioned methods is described in detail elsewhere [2].

The elemental analysis of feedstock samples was determined in a LECO CHNS-932 (C, H, N, S) and LECO VTF-9000 (O) analyzers. Proximate analysis, in terms of volatile matter, moisture and ash content, was performed in a LECO TGA-601 analyzer. Mineral matter composition was determined by means of X-ray fluorescence in a Bruker SRS 3000 analyser.

The reactivity of the fuel mixtures was assessed by thermogravimetric analysis in a Q5000 IR (TA Instruments) thermobalance. The mass loss profile of 10 mg of sample was monitored by increasing the temperature up to 1000 °C with 10 °C/min, under either N_2 (inert) or CO_2 (reactive) atmosphere. Thus, the mass loss is attributed to the single effect of temperature in the case of nitrogen flow, whereas in the case of CO_2 atmosphere its interaction with carbon further contributes to weight loss.

2.4 DCFC fabrication and testing

The DCFC electrochemical tests were performed under batch mode of operation in the reactor cell, schematically illustrated in Fig.1, consisting of an YSZ electrolyte tube (15 cm length, I.D.=16mm, 1.5mm thickness), metallic silver (Ag) as cathode and Co/CeO_2 as anode, with the latter having a layer thickness ranging between 10 and 40 μm.

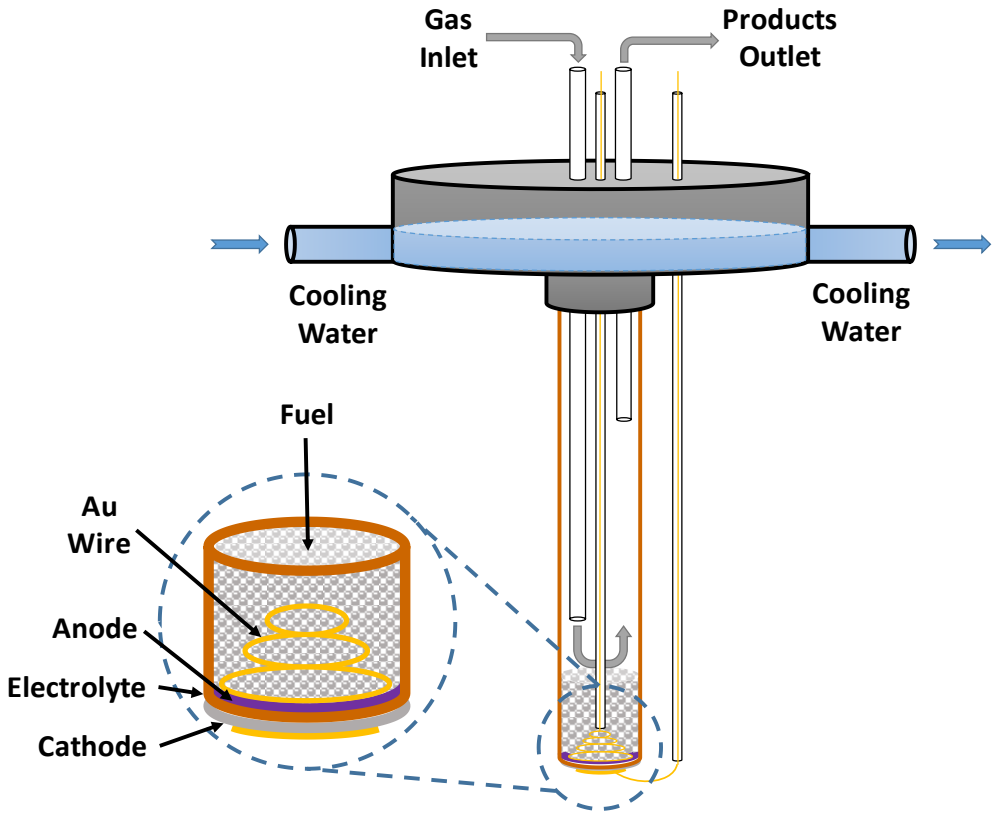

Fig. 1. DCFC schematic representation.

Silver (Ag) was selected as cathode electrode since it is known to improve the oxygen exchange reaction activity [44]. Ag-containing electrodes have shown high activity towards oxygen reduction reaction making Ag as an efficient and promising component for SOFC cathodes [45-47]. The experimental details in relation to fuel cell fabrication are provided in our previous works [2, 13, 21, 25, 35, 43].

Prior to electrochemical measurements, the cell was initially loaded with different fuel feedstock, *i.e.*: (i) 800 mg of carbon or (ii) 800 mg carbon + 400 mg catalyst or (iii) 800 mg carbon + 200 mg carbonates or (iv) 800 mg carbon + 400 mg catalyst + 200 mg carbonates in order to assess the individual or synergistic effect of the different components. During the DCFC testing, pure CO_2 (Air Liquide) was continuously fed at the anode chamber with a feed flow rate of 30 cm^3/min at STP conditions. A gas chromatograph (Shimadzu GC-14B) was employed to monitor the anode effluent stream at open and closed circuit conditions.

The electrochemical measurements were carried out at 700, 750 and 800 °C under ambient pressure. The voltage-current density measurements and the AC impedance spectroscopy studies were carried out by means of a Versa Stat 4 electrochemical station (Princeton Applied Research) aided by Versa Studio software. The impedance spectra were modeled with the Z-view software (Scribner Associates), according to the equivalent circuit presented in Fig. 2.

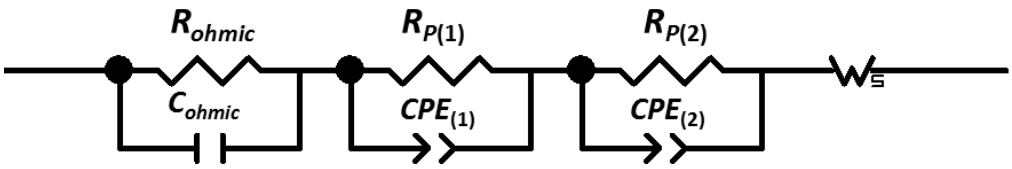

Fig. 2. Equivalent circuit with ohmic resistance (R_{ohmic}) and capacitance (C_{ohmic}) and three contributions of the electrode resistance, $R_{P(1)}$, $R_{P(2)}$ and Ws. $R_{P(1)}$ and $R_{P(2)}$ are dencovoluted with the corresponding constant phase elements $CPE_{(1)}$ and $CPE_{(2)}$, standing for double layer and mass transfer pseudo-capacitances, respectively. The Warburg element accounts for additional mass transport contribution.

3. RESULTS AND DISCUSSION

3.1 Physicochemical characterization of fuel feedstock

The coal used in the present study is a bituminous coal (BC) from Spanish basin. Its particle size distribution (PSD) obtained after milling and subsequent sieving is depicted in Figure 3, revealing particles lower than ca. 50 microns. This specific coal was selected, as already mentioned, based on its high carbon content (*i.e.*, 90 wt.% in dry ash free basis) and low ash content (*i.e.*, 4.1 wt%). The proximate analysis and elemental composition of the mineral coal as well as of its mixtures with catalyst and/or carbonates are shown in Table 1.

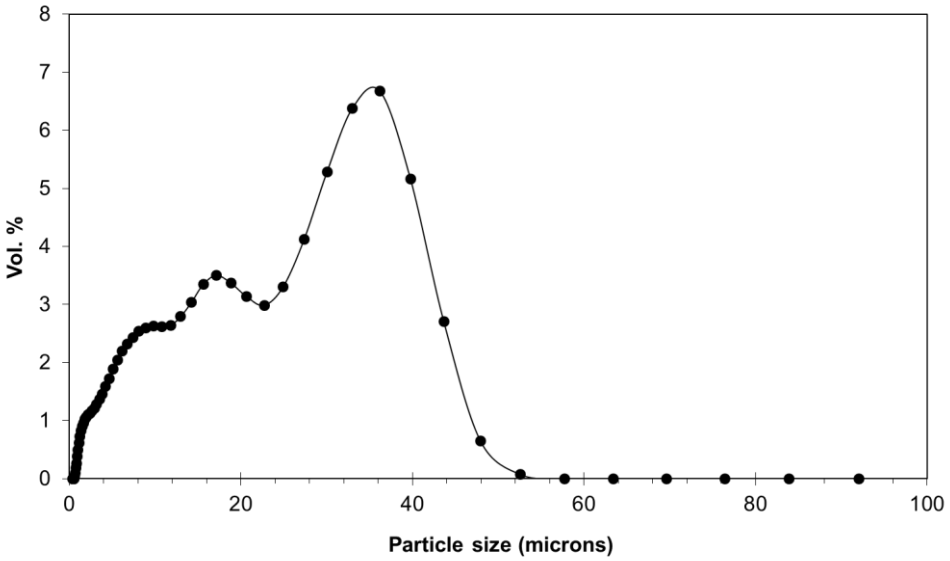

Fig. 3. Particle size distribution of the bituminous coal.

Table 1: Proximate and elemental analysis of the different feedstock employed.

Feedstock	Proximate Analysis (wt.%)			Ultimate Analysis (wt.%, dry ash free basis)				
	Volatile content	Inorganic matter	Moisture	C	H	N	S	O
carbon	18.1	4.1	0.9	90.0	4.8	1.7	0.0	3.5
carbon/catalyst	14.5	25.0	1.1	83.6	4.5	1.8	0.0	10.1
carbon/carbonates	28.7	12.5	1.4	82.0	4.3	1.6	0.0	12.1
carbon/catalyst/carbonates	24.3	33.5	0.7	79.6	4.3	1.7	0.0	14.4

In Table 2 the composition of the bituminous coal inorganic matter is presented. The mineral matter analysis indicates that BC is mainly composed from Al (~30 wt.%), Si (~50 wt.%) and Fe (~10 wt.%) compounds, while minor amounts from Na, Mg, P, K, and Ti (of a total ca. 10 wt.%) were also determined. These impurities are expected to have a different impact on the DCFC performance, depending on their effect on cell materials as well as on the overall electro-chemical reaction network. In this regard, it has been reported that Al_2O_3 and SiO_2 have an inhibiting role, whereas CaO, MgO, Fe_2O_3 exhibit in general a pronounced catalytic effect [20].

Table 2: Inorganic matter content of the BC (wt.%).

Na_2O	**MgO**	**Al_2O_3**	**SiO_2**	**P_2O_5**	**K_2O**	**CaO**	**TiO_2**	**Fe_2O_3**
1.2	1.0	30.3	48.7	2.3	2.3	2.6	1.8	9.8

As can be seen in Table 1, the incorporation of catalyst and carbonates into carbon increases the inorganic matter from 4.1 wt.% over the bare BC to 12.5, 25 and 33.5 wt.% for carbon/carbonates, carbon/catalyst and carbon/catalyst/carbonates mixtures, respectively. This is due to the fact that the Co/CeO_2 composite is just an inorganic matter, whereas carbonates may be decomposed generating CO_2 that contributes to the volatile matter loss as well as to a surplus residue contributing to the increase of inorganic matter. The ultimate analysis shows that the BC has negligible sulfur content, which is notably advantageous considering the degradation effect of sulfur in DCFC performance [2, 13, 31-34, 42]. Interestingly, the oxygen content is notably increased by catalyst and/or carbonates infusion to carbon feedstock. The latter is of particular importance towards the facilitation of carbon gasification processes in anode compartment, as will be discussed below.

It is worth to note that the volatile content (*i.e.*, loss of matter in inert atmosphere at 800 ºC) increases mainly due to the presence of carbonates, which are decomposed evolving CO_2. The evolved CO_2 contributes to the mass loss of the mixture whereas in addition partially reacts with the coal increasing the organic material losses. If the catalyst is considered just as an inorganic matter whereas carbonates as a partially volatile matter (*i.e.*, CO_2 is evolved during carbonates decomposition by increasing the temperature) and a residual inorganic matter, the theoretical estimated volatile composition of the carbon/catalyst, carbon/carbonates and carbon/catalyst/carbonates samples is ca. 12, 23 and 17 wt.%, respectively. It can be observed that the proximate analysis shows higher values for the volatile content (*i.e.*, 15, 29 and 24 wt.%, respectively), probably due to the interaction of catalyst and

carbonates with the organic matter during thermal decomposition. Therefore, the addition of catalyst and carbonates promotes volatile evolution of the mineral coal, which is expected to favor the DCFC electrochemical performance. These observations are also corroborated by the thermogravimetric analysis of the different feedstock mixtures, by heating up to 1000 ºC in inert (20 ml/min of N_2) and reactive (20 ml/min CO_2) atmospheres, as shown in Fig. 4.

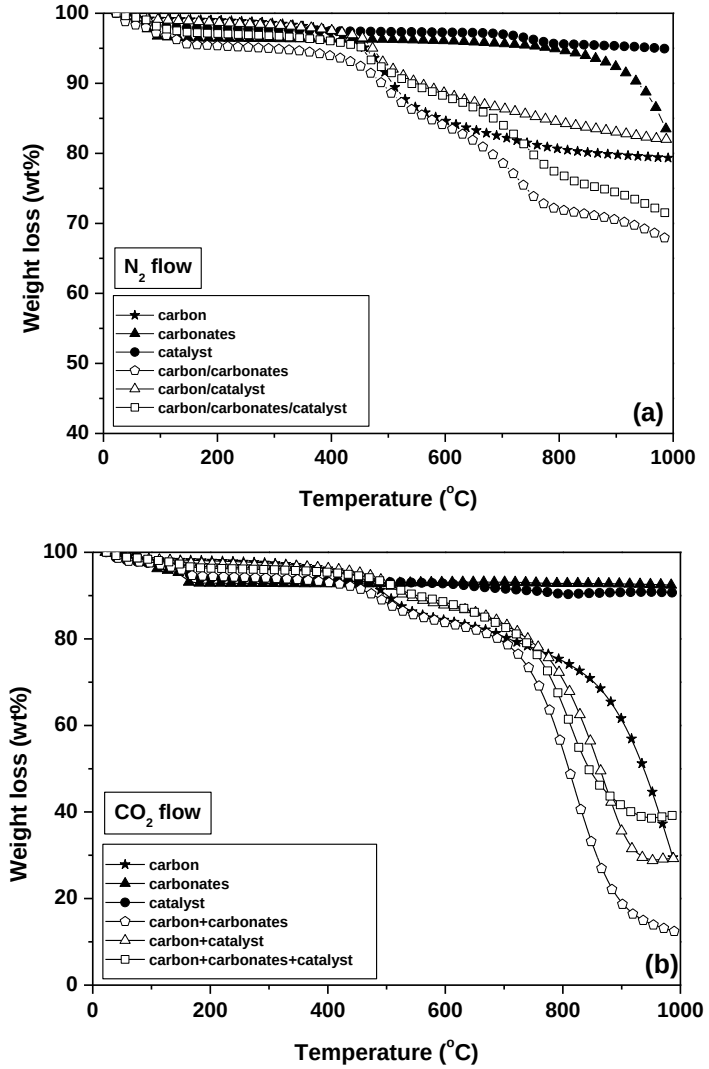

Fig. 4. Weight loss profiles of the different fuel feedstock in (a) inert (N_2) and (b) reactive (CO_2) atmospheres.

It can be observed that catalyst is not thermally decomposed (Fig. 4a), whilst the carbonates are decomposed at temperatures higher than 700 ºC. Catalyst addition does not affect the carbon weight loss profile under inert atmosphere. However, carbonates addition increases the weight loss of the coal above 600 ºC, probably because part of the CO_2 generated during carbonates decomposition gasifies the coal sample. On the other hand, under reactive (CO_2) atmosphere (Fig. 4b), it is clearly

shown that the addition of catalyst notably increases the weight loss of carbon both in the absence and presence of carbonates. This behavior can be ascribed to the catalyst-aided rBR towards carbon gasification to CO (eq. 8). The addition of carbonates can further promote the rBR *via* their decomposition to CO_2 and its subsequent interaction with carbon. Hence, a synergistic catalyst/carbonate effect towards carbon gasification is expected. However, it is interesting to note that the bare carbonates sample is not decomposed under CO_2 atmosphere, since the presence of 100 v/v% CO_2 shifts the equilibrium of carbonates decomposition reaction to reactants (Fig. 4b). Table 3 summarizes the wt.% loss of the different feedstock mixtures and of their different counterparts under inert (N_2) and reactive (CO_2) atmosphere, obtained by thermogravimetric analysis. The results are in agreement with the proximate analysis of the samples shown in Table 1.

Table 3: Weight loss of the different feedstock mixtures and their counterparts (bituminous coal= C; catalyst= CAT; carbonates= CB) obtained by thermogravimetric analysis under inert (N_2) and reactive (CO_2) atmosphere.

TGA Atmosphere	**C (wt.%)**	**CAT (wt.%)**	**CB (wt.%)**	**C+CB (wt.%)**	**C+CAT (wt.%)**	**C+CB+CAT (wt.%)**
N_2	21	5	17	32	18	28
CO_2	71	9	7	88	71	61

The textural characterization of the samples by N_2 adsorption-desorption isotherms shows that the bituminous coal has negligible pore volume and surface area. On the other hand, the carbon/carbonates mixture possesses a surface area of ca. 10 m^2/g with an overall pore volume of 0.02 cm^3/g. Carbon/catalyst mixture presents the optimum textural characteristics with 18 m^2/g BET area and 0.06 cm^3/g total pore volume, while intermediate values, *i.e.*, 16 m^2/g surface area and 0.05 cm^3/g pore volume were obtained for carbon/catalyst/carbonate mixture.

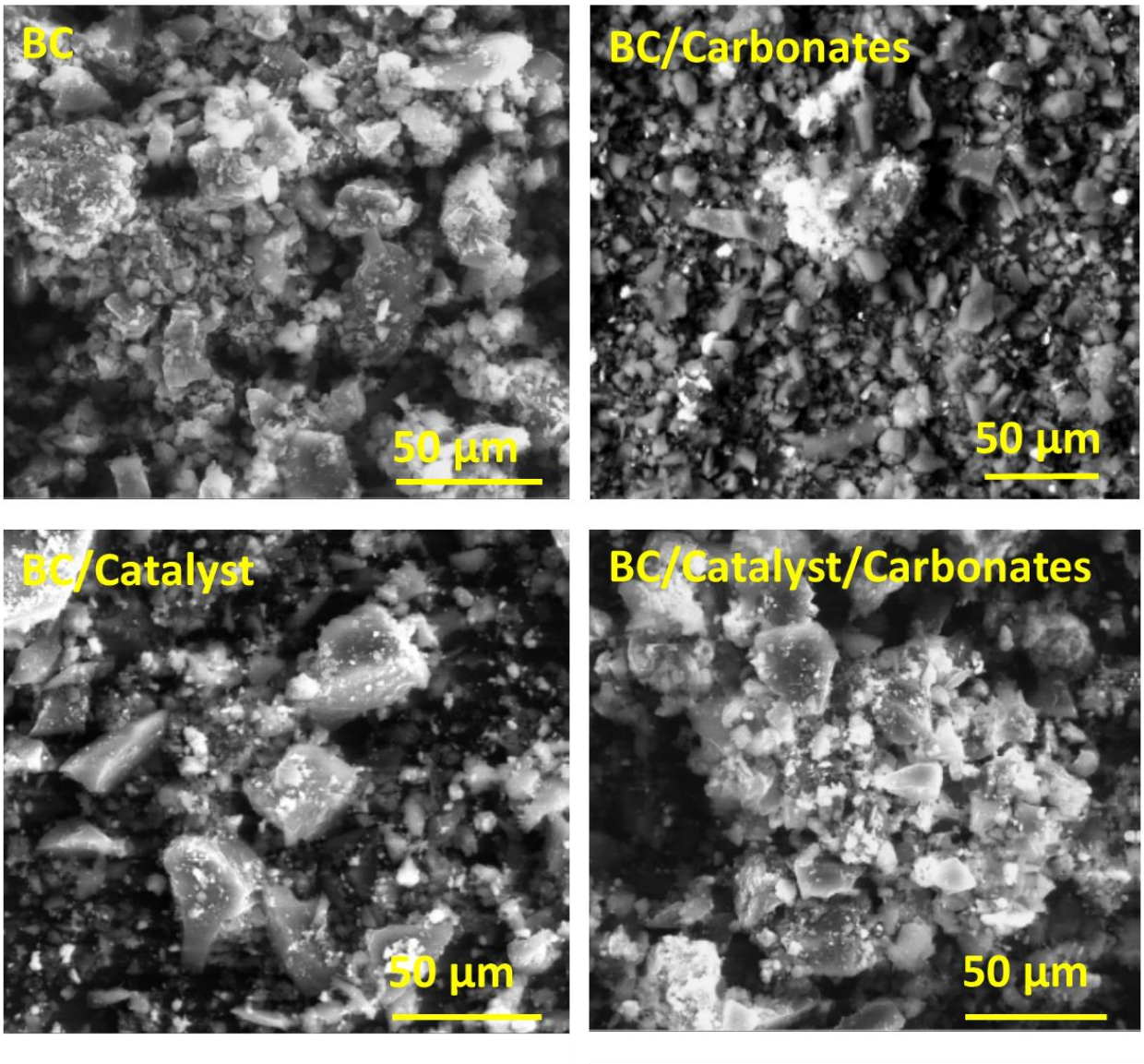

Fig. 5. SEM pictures of the bituminous coal and of the different fuel mixtures.

Representative SEM images of the different feedstock mixtures are shown in Fig. 5. In the corresponding pictures of the binary and ternary mixtures, the white spots are attributed to the catalyst and carbonates particles as well as to the mineral matter in the pristine bituminous coal sample, which however cannot be clearly distinguished from the inorganic catalyst and carbonates particles. The samples show a uniform distribution of the different counterparts as further verified by EDX analysis, which performed in different points/areas, always implying a homogeneous composition. An indicative EDX analysis for the BC/Catalyst mixture is shown in Figure 6.

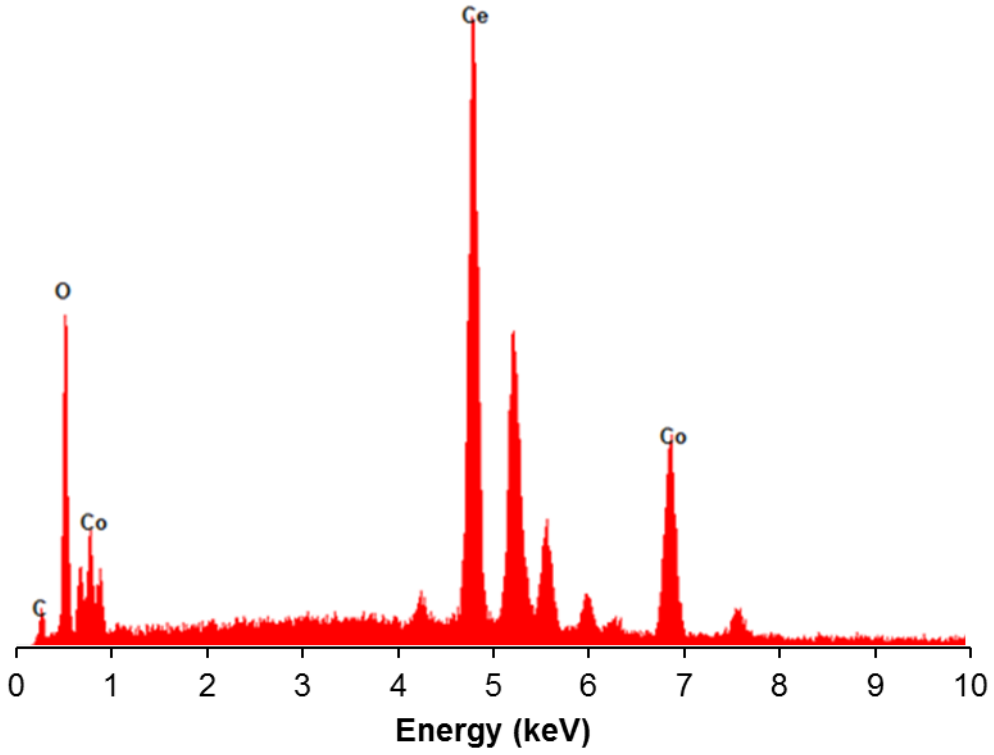

Fig. 6. EDX analysis of the carbon/catalyst feedstock mixture.

The XRD spectra of the different fuel mixtures are depicted in Fig. 7. Bituminous coal presents the typical features of carbon structure, with a wide peak at ca. 25º corresponding to the condensed aromatic rings of coal structure. It has to be noted that the present bituminous coal has very low mineral matter content (4 wt.%) so it is difficult to identify the mineral components by this technique, as the signal corresponding to the carbonaceous structure masks other minor signals. In this regard, the mineral matter composition of BC sample was determined by X-ray fluorescence analysis, as shown in Table 2. The corresponding XRD spectra of the carbonates mixture (Li_2CO_3/K_2CO_3) and the catalyst (Co/CeO_2) were also incorporated in Fig. 7, as reference spectra. It can be seen that the carbon/carbonates mixture presents a less intense signal for carbonaceous structure besides some well-defined peaks from carbonates, mainly from Li_2CO_3. In addition, the carbon/catalyst feedstock shows an even less intense signal for carbonaceous counterpart in addition to some very well defined peaks from CeO_2. Finally, the ternary mixture presents a very low signal for carbon structure with some low intensity peaks corresponding to CeO_2 and carbonates. These findings are confirming the results obtained from SEM-EDX mentioned above, indicating that the different counterparts in the

binary and ternary feedstock mixtures present a uniform distribution with a homogeneous composition.

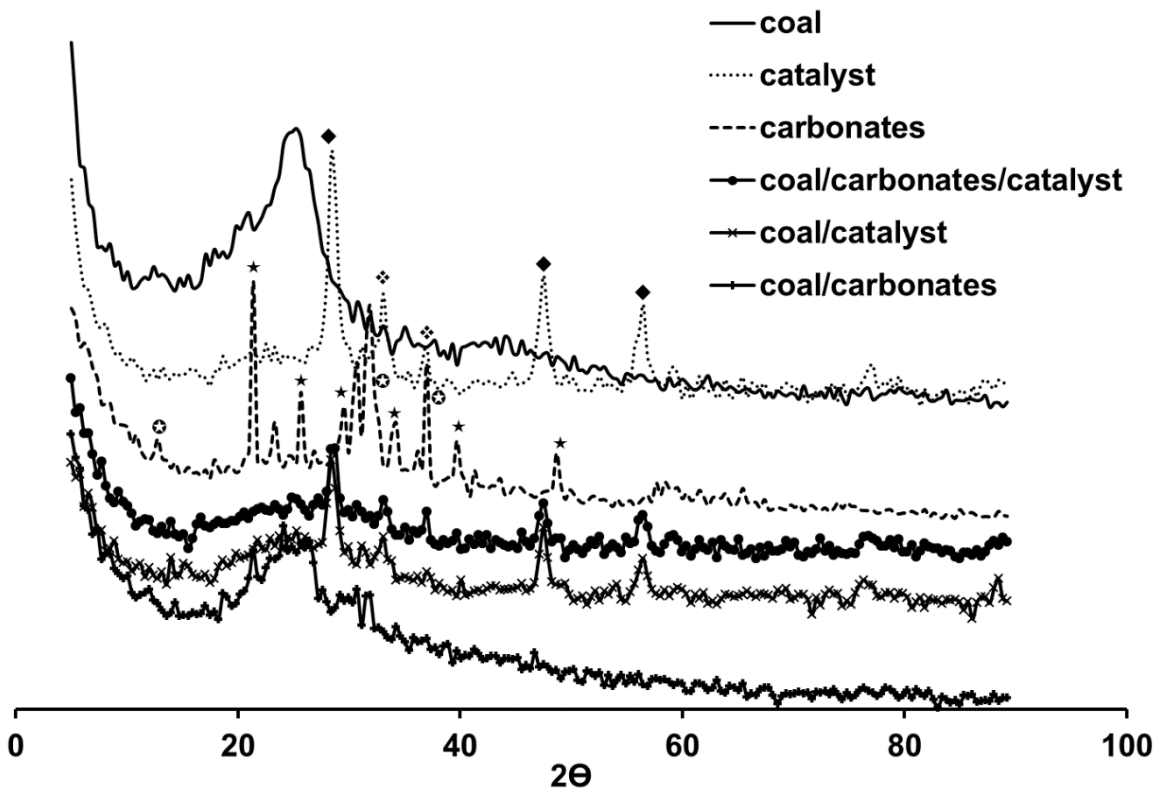

Fig. 7. XRD diffractograms of the different fuel feedstock studied.
(Note: ◆=CeO_2; ❖=Co_3O_4; ✪=K_2CO_3; ★=Li_2CO_3).

3.2 DCFC electrochemical testing

3.2.1 Impact of catalyst infusion on cell performance in the absence of carbonates

Fig. 8 depicts the effect of Co/CeO_2 addition on the DCFC electrochemical performance, employing CO_2 as gasifying agent. The beneficial effect of catalyst on the power output is obvious at all temperatures investigated; an increment on the power density up to 20% is attained by catalyst infusion to carbon fuel (Table 4). A similar positive trend was also observed in our previous work upon catalyst incorporation to different coals and charcoal fuels, with the increase in DCFC performance to be more intense at lower cell temperatures and for the less reactive samples [2].

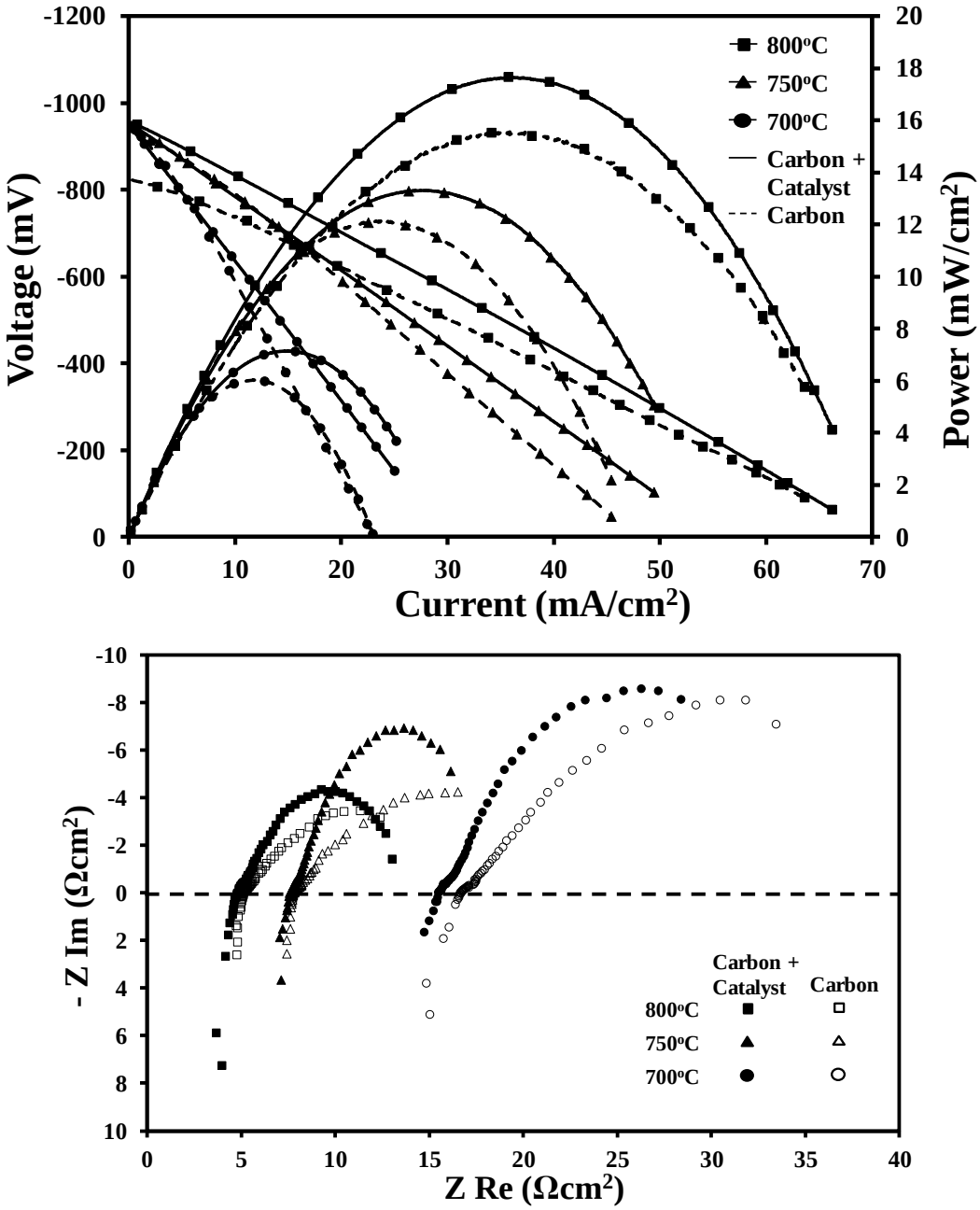

Fig. 8. Effect of catalyst infusion on cell characteristics and AC impedance spectra at identical conditions. Feedstock: 800 mg bituminous coal (+ 400 mg catalyst); T= 700-800 °C; CO_2 flow rate= 30 cm^3/min.

Deleebeeck *et al.* [27] also observed an increase in the DCFC electrochemical performance by incorporating Mn_xO_y catalyst into bituminous coal, with 73 mW/cm^2 maximum power density at 755 °C. In a similar manner, Rady *et al.* [26] found that the infusion of Ca and Fe particles in carbon black

(Vulcan XC-72) resulted in an enhancement of maximum power density to 49 and 36 mW/cm^2 at 850 ^{o}C, respectively, as compared to 26 mW/cm^2 with bare carbon. Similar results were also obtained by employing activated carbon as fuel in catalyst-aided DCFC experiments [28, 29].

Table 4: CO production rate at OCV and maximum power density. Bituminous coal loading= 800 mg; carbon/catalyst/carbonate weight ratio= 4/2/1.

Temperature (^{o}C)	Feedstock composition							
	Carbon		Carbon/Catalyst		Carbon/Carbonate		Carbon/Catalyst/ Carbonate	
	r_{CO} at OCV (10^{-8} mol/s)	P_{max} (mW/cm^2)	r_{CO} at OCV (10^{-8} mol/s)	P_{max} (mW/cm^2)	r_{CO} at OCV (10^{-8} mol/s)	P_{max} (mW/cm^2)	r_{CO} at OCV (10^{-8} mol/s)	P_{max} (mW/cm^2)
700	10.9	6.0	14.2	7.2	24.1	7.7	27.0	10.9
750	12.3	12.2	15.9	13.6	27.3	15.3	30.9	19.5
800	14.5	15.5	18.8	17.7	31.9	20.2	35.8	24.7

Fig. 8 also presents the corresponding AC impedance measurements. It is clearly shown that both the ohmic and polarization resistances are lowered upon cell temperature increase and Co/CeO_2 addition into carbon fuel, justifying the pronounced effect of temperature and catalyst infusion on the DCFC electrochemical characteristics (Fig. 8). In specific, the ohmic resistance for the bare bituminous DCFC experiments equals to 16.7 Ω cm^2 at 700 ^{o}C and is decreased to 5.1 Ω cm^2 at 800 ^{o}C, revealing the beneficial effect of temperature on ohmic resistance, while the corresponding values in the co-presence of Co/CeO_2 catalyst are slightly lowered, *i.e.*, 15.8 and 4.77 Ω cm^2, respectively. The positive impact of operating temperature on ohmic resistance is evident, while the corresponding slight decrease upon catalyst addition can be attributed to the anode reduction induced by the *in situ* formed CO *via* the rBR [43]. In a similar manner, the electrode polarization resistance (R_P) – here defined as the sum of three partial contributions arising from charge and mass transfer processes (R_P = $R_P(1)$ + $R_P(2)$ +W_S-R) at the electrodes – is decreased by increasing cell temperature and upon catalyst addition. R_P in the absence of catalyst is equal to 23.6 Ω cm² at 700 ^{o}C and decreases substantially to 9.6 Ω cm² at 800 ^{o}C, whereas in the case of catalyst-aided DCFC experiments the corresponding values are equal to 17 and 9.5 Ω cm², respectively.

More specifically, the feature of AC impedance spectra is consisted of three overlapping arcs. The first one at high frequencies ($R_{P(1)}$ in Figure 2) with an associated capacitance in the order of mF/cm^2 representing the corresponding carbon and CO oxidation charge transfer processes. The overlapped second arc ($R_{P(2)}$ in Figure 2) has a higher associated capacitance in the order of 10^{-2} F/cm^2 and it can

be assigned to mass transfer processes involving gaseous or solid species presented in the anode chamber. The third part of the electrode arc, contributing at low frequencies is characteristic of a Warburg element, also this reflecting a contribution from mass transfer processes in the anode compartment. By the analysis of the individual contributions it seems that the major part of electrode polarization resistance is assigned to mass transfer limitations of combustible gaseous species (CO, H_2, CH_4) and of solid carbon to anode solid electrolyte/electrode interface. In addition, it should be noted that in the case of bare bituminous coal, $R_{P(2)}$ is larger compared to the low frequency Warburg resistance. The two contributions are indistinguishable in the catalytic DCFC experiments. This behavior can be probably attributed to the inhibiting role of catalyst presence on the diffusion of solid fuel particles into the electrode/electrolyte interface.

3.2.2 Combined impact of catalyst and carbonates on DCFC performance.

An eutectic mixture of carbonates was mixed with either bituminous or bituminous/catalyst feedstock at a carbon/catalyst/carbonate weight ratio of 4:2:1, to examine the individual effect of carbonates as well as the possible synergistic effect of catalyst and carbonates on DCFC performance. The beneficial effect of carbonates addition into bituminous and bituminous/catalyst mixture on the DCFC characteristics is shown in Fig. 9. Specifically, carbonates infusion to carbon and carbon/catalyst feedstock results in a power increment up to ca. 30 and 50 %, respectively, as compared to the obtained maximum power density for bare carbon (Table 4). In specific, a maximum power density of 24.7 mW/cm^2 at 800 ^{o}C was achieved in the case of carbon/catalyst/carbonates feedstock mixture compared to 20.2, 17.7 and 15.5 mW/cm^2 for the carbon/carbonates, carbon/catalyst and bare carbon feedstock, respectively. These values are higher compared to those obtained in a similar system with Cu/CeO_2 as anode electrode and carbon black as fuel [25], but lower compared to other similar studies where bituminous coal was also investigated as fuel. For instance, Jiang *et al.* [42] observed a maximum power density of 42 mW/cm^2 at 750 °C (NiO-YSZ|YSZ|LSM-(LK)CO_3), while Chen *et al.* [48] achieved 165 mW/cm^2 at 700 °C (|NiO-YSZ|YSZ|LSM-YSZ|) using bituminous coal as fuel. The differences can be mainly assigned to the higher ohmic and concentration losses observed in the present study as compared to the aforementioned works [42, 48].

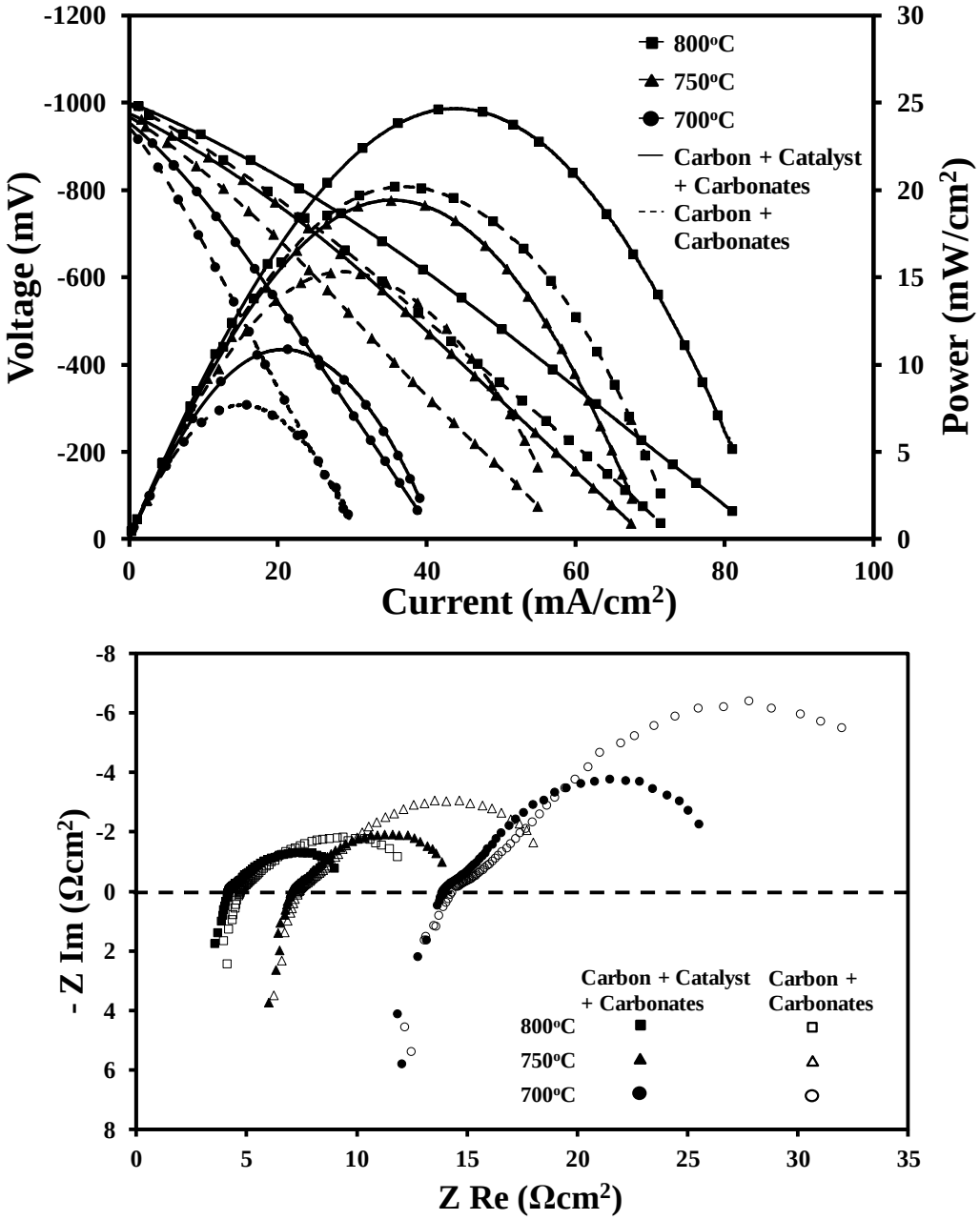

Fig. 9. Effect of catalyst and/or carbonates infusion on cell characteristics and AC impedance spectra at identical conditions. Feedstock: 800 mg bituminous coal, (+ 200 mg carbonates), (+ 400 mg catalyst); T= 700-800 °C; CO_2 flow rate=30 ml/min.

By analyzing the corresponding impedance data, it is revealed that the ohmic resistance is decreased upon carbonates addition in the fuel mixture, from 16.7, 7.7 and 5.1 Ω cm^2 for bare coal to 14.2, 7.3 and 4.7 Ω cm^2 for coal/carbonates mixtures, at 700, 750 and 800 ºC, respectively. A further

improvement of ohmic resistance is observed in the case of ternary carbon/catalyst/carbonate feedstock, where the corresponding ohmic resistance values are decreased to 14.0, 7.0 and 4.2 Ω cm^2. Carbonates addition in the fuel mixture results in a lower polarization resistance, whereas a more drastic decrease is achieved by the co-addition of carbonates and catalyst to carbon fuel. In the case of carbon/carbonates mixture, the electrode polarization resistance is 22.5, 12.0 and 7.6 Ω cm^2, while for the carbon/catalyst/carbonates feedstock it is decreased to 13.0, 7.7 and 5.5 Ω cm^2 at 700, 750 and 800 °C, respectively. It clearly appears that the electrode polarization resistance decreases with temperature. Furthermore, R_p is lowered in the presence of carbonates, mainly by reducing the resistance due to mass transfer limitations which continue to dominate over the corresponding contribution by the charge transfer processes. This behavior is attributed to the beneficial effect of carbonates on the fluidity of solid carbon toward the anode TBP, as well as to the enhancement of rBR process by the surplus CO_2 generated by the decomposition of carbonates, as revealed by the TGA experiments (Fig. 4). This additional CO_2 gives rise to the formation rate of CO, which exhibits better mass transport and faster electrode kinetics compared to BC.

Summarizing, the present results clearly demonstrate the beneficial impact of catalyst infusion to direct carbon or hybrid carbon/carbonates fuel cells. More specifically, a synergistic catalyst-carbonate effect towards improving the cell efficiency is revealed, as obviously shown in Fig. 10. These findings can be well understood by taking into account the key role of carbonates and catalyst on carbon diffusion as well as on the formation of CO *via* the rBR (eq. 8) or the carbon-carbonates reactions (eqs. 6 and 7). In particular, carbonates facilitate the diffusion of bituminous coal while at the same time provide additional CO_2 through their thermal decomposition, which is interacting with solid carbon, bypassing indirectly the associated mass transfer limitations. At the same time, in the presence of catalyst, although the rBR is enhanced and additional CO is produced, its presence may interfere with the coal fluidity at the anode. However the simultaneous use of catalyst and carbonates has clearly a beneficial effect resulting in higher power densities and better DCFC electrochemical performance, compared to bare bituminous coal DCFC experiments.

It should be also mentioned, that the *in situ* generated CO notably improves the DCFC characteristics as CO diffuses more rapidly to anode TBP and presents better electro-kinetics in comparison to bare carbon. The above arguments are totally supported by the close relationship between the open circuit CO formation rate at each temperature and the achieved maximum power output (P_{max}), as depicted in Table 4. The key role of *in situ* formed CO on DCFC performance has been extensively discussed

[2, 8, 13, 14, 21, 24, 25, 28, 35, 43]. Moreover, AC impedance spectroscopy experiments accompanied with GC measurements clearly revealed the beneficial impact of *in situ* generated CO on ohmic and electrode polarization resistances [2, 43].

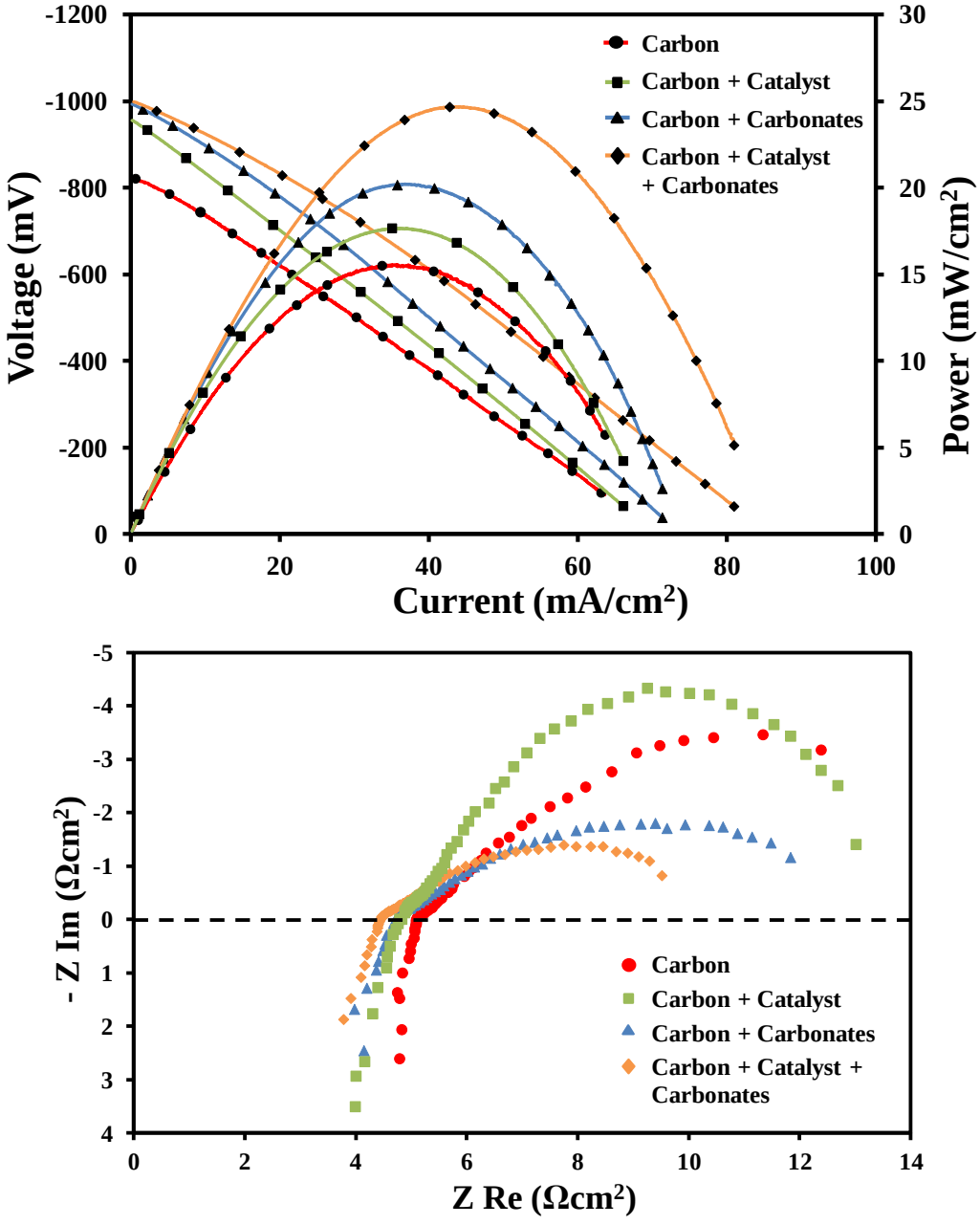

Fig. 10: Electrochemical performance of catalyst-aided DCFC and HDCFC configurations at 800 °C and the corresponding AC impedance spectra at identical conditions. Feedstock: 800 mg bituminous coal, (+ 200 mg carbonates), (+ 400 mg catalyst); CO_2 flow rate= 30 ml/min.

The proposed approach of catalyst/carbonates infusion to fuel feedstock substantially improves the DCFC performance. Such technological advancements could notably accelerate DCFCs market roll out. The latter could be of particular importance taking into account the major benefits of DCFC technology compared to conventional coal power plants, such as the high electrical efficiency and low environmental footprint. However it should be noted that the achieved maximum power densities are relatively low due to the large ohmic and concentration overpotentials ascribed mainly to the high thickness of the YSZ solid electrolyte and the low porosity of the anode layer, respectively, as well as to cell configuration issues such as the current collection set up [49]. In this direction, Lee et al. found that the modification of the anode microstructure by the incorporation of poly(methyl mathacrylate) (PMMA) pore-formers resulted to a substantial increase in the achieved maximum power density [24]. In addition, in the work of Gil et al., a cathode supported planar cell configuration led to an improved DCFC performance [50]. Therefore, research efforts are currently in progress to decrease the wall thickness of YSZ tube and modify the fabrication protocol of the anode film in order to improve the obtained DCFC electrochemical performance.

4. CONCLUSIONS

In the present work, the feasibility to improve the DCFC performance by infusing a gasification catalyst (Co/CeO_2) and/or carbonates into the bituminous coal feedstock was systematically examined. The maximum power density is enhanced up to 20%, 30% and 80%, for carbon/catalyst, carbon/carbonates and carbon/catalyst/carbonates fuel mixtures, respectively, compared with bare bituminous coal DCFC experiments. The obtained findings can be well interpreted taking into account the pronounced effect of catalyst/carbonates on the solid fuel fluidity and the rBR; the *in situ* generated CO can be rapidly diffused to the anode TBP, offering faster electrochemical oxidation kinetics as compared to solid coal. In view of this fact, a close relationship between the CO production rate and the maximum DCFC power was established. The present results originally demonstrate the beneficial role of catalyst as well as the catalyst-carbonate synergy towards the improvement of cell performance.

Acknowledgements

This research has been co-financed by the European Union and Greek national funds through the Operational Program Competitiveness, Entrepreneurship and Innovation, under the call RESEARCH – CREATE – INNOVATE (project code: T1EDK-01894).

Dr. Kaklidis' postdoctoral research was realized via the framework of "Grant Allowance for Post-Doctoral Researchers" of the operational programme "Human Resources Development, Education and Lifelong Learning", 2014-2020, implemented by the State Scholarships Foundation (IKY) and co-funded by the European Social Fund and the Hellenic state.

RERERENCES

[1] BP Statistical Review of World Energy, 67th Edition, June 2018. https://www.bp.com/content/dam/bp/en/corporate/pdf/energy-economics/statistical-review/bp-stats-review-2018-full-report.pdf.

[2] Konsolakis M., Kaklidis N., Kyriakou V., Garagounis I., Kraia Tz., Arenillas A., Menendez J.A., Strandbakke R., Marnellos G.E. (2018). The combined impact of carbon type and catalyst-aided gasification process on the performance of a Direct Carbon Solid Oxide Fuel Cell. *Solid State Ionics*, 317, 268-275.

[3] Badwal, S.P.S., Ju, H., Giddey, S., Kulkarni, A. (2017). Direct Carbon Fuel Cells. Book chapter in Encyclopedia of Sustainable Technologies, 317-329.

[4] Jiang C., Ma J., Corre J. Jain S.L., Irvine J.T.S. (2017). Challenges in developing direct carbon fuel cells, *Chemical Society Reviews*, 46(10), 2889-2912.

[5] Deleebeeck L., Hansen K.K. (2014). Hybrid direct carbon fuel cells and their reaction mechanisms. *Journal of Solid State Electrochemistry*, 18(4), 861-862.

[6] Gür, T.M. (2013). Critical review of carbon conversion in "carbon fuel cells". *Chemical Reviews*, 113(8), 6179-206.

[7] Giddey, S., Badwal, S.P.S., Kulkarni, A., Munnings, C. (2012). A comprehensive review of direct carbon fuel cell technology. *Progress in Energy and Combustion Science*, 38(3), 360-99.

[8] Li J., Wei B., Wang Ch., Zhou Z., Lu Z. (2018). High-performance and stable $La_{0.8}Sr_{0.2}Fe_{0.9}Nb_{0.1}O_{3-\delta}$ anode for direct carbon solid oxide fuel cells fueled by activated carbon and corn straw derived carbon. *International Journal of Hydrogen Energy*, 43(27), 12358-12367.

[9] Li S., Pan W., Wang S., Meng X., Jiang C., Irvine J.T.S. (2017). Electrochemical performance of different carbon fuels on a hybrid direct carbon fuel cell. *International Journal of Hydrogen Energy*, 42(25), 16279-16287.

[10] Lee C.-G. Kim W.-K. (2015). Oxidation of ash-free coal in a direct carbon fuel cell. *International Journal of Hydrogen Energy*, 40(15), 5475-5481.

[11] Munnings C., Kulkarni A., Giddey S., Badwal S.P.S. (2014). Biomass to power conversion in a direct carbon fuel cell. *International Journal of Hydrogen Energy*, 39(23), 12377-12385.

[12] Elleuch A., Boussetta A., Yu J., Halouani K., Li Y. (2013). Experimental investigation of direct carbon fuel cell fueled by almond shell biochar: Part I. Physico-chemical characterization of the biochar fuel and cell performance examination. *International Journal of Hydrogen Energy*, 38(36), 16590-16604

[13] Kaklidis, N., Kyriakou, V., Garagounis, I., Arenillas, A., Menendez, J. A., Marnellos G. E., Konsolakis, M., (2014). Effect of carbon type on the performance of a direct or hybrid carbon solid oxide fuel cell. *RSC Advances*, 4(36), 18792–18800.

[14] Jewulski J., Skrzypkiewicz M., Struzik M., Lubarska-Radziejewska I. (2014). Lignite as afuel for direct carbon fuel cell system. *International Journal of Hydrogen Energy*, 39, 21778-21785.

[15] Jafri N., Wong W.Y., Doshi V., Yoon L.W., Cheah K.H. (2018). A review on production and characterization of biochars for application in direct carbon fuel cells. *Process Safety and Environmental Protection*, 118, 152-166.

[16] Dudek M., Tomczyk P., Socha R., Hamaguchi M. (2014). Use of ash-free "Hyper –coal" as a fuel for a direct carbon fuel cell with solid oxide electrolyte. *International Journal of Hydrogen Energy*, 39, 12386-12394.

[17] Liu G., Zhang Y., Cai J., Zhou A., Dang Y., Qiu J. (2018). A strategy for regulating the performance of DCFC with semi-coke fuel. *International Journal of Hydrogen Energy*, 43, 7465-7472.

[18] Liu, J., Zhou, M., Zhang, Y., Liu, P., Liu, Z., Xie, Y., Cai, W., Yu, F., Zhou, Q., Wang, X., Ni, M., Liu, M. (2018). Electrochemical Oxidation of Carbon at High Temperature: Principles and Applications. *Energy and Fuels*, 32(4), 4107-4117.

[19] Liu, G.-Y., Zhang, Y.-T., Cai, J.-T., Zhang, X.-Q., Qiu, J.-S. (2015). Fuels for direct carbon fuel cells: Present status and development prospects. *New Carbon Materials*, 30(1), 12-18.

[20] Rady, A.C., Giddey, S., Badwal, S.P.S., Ladewig, B.P., Bhattacharya, S. (2012). Review of fuels for direct carbon fuel cells. *Energy and Fuels*, 26(3), 1471-1488.

[21] Konsolakis, M., Kaklidis, N., Marnellos, G.E., Zaharaki, D., Komnitsas, K. (2015). Assessment of biochar as feedstock in a direct carbon solid oxide fuel cell. *RSC Advances*, 5, 73399-73409.

[22] Dudek, M. (2015). On the utilization of coal samples in direct carbon solid oxide fuel cell technology. *Solid State Ionics*, 271, 121-127.

[23] Li, X., Zhu, Z., De Marco, R., Bradley, J., Dicks, A. (2010). Evaluation of raw coals as fuels for direct carbon fuel cells. *Journal of Power Sources*, 195(13), 4051-4058.

[24] Lee J.-Y., Song R.-H., Lee S.-B., Lim T.-H., Park S.-J., Shul Y.G., Lee J.-W. (2014). A performance study of hybrid direct carbon fuel cells: Impact of anode microstructure. *International Journal of Hydrogen Energy*, 39, 11749-11755.

[25] Konsolakis, M., Marnellos, G.E., Al-Musa, A., Kaklidis, N., Garagounis, I., Kyriakou, V. (2015). Carbon to electricity in a solid oxide fuel cell combined with an internal catalytic gasification process. *Chinese Journal of Catalysis*, 36, 509-516.

[26] Rady, A.C., Giddey, S., Kulkami, A., Badwal, S.P.S., Bhattacharya, S. (2016). Catalytic gasification of carbon in a direct carbon fuel cell. *Fuel*, 180, 270-277.

[27] Deleebeeck L., Ippolito, D., Kammer Hansen, K. (2015). Catalytic enhancement of carbon black and coal-fueled hybrid direct carbon fuel cells. Journal of the Electrochemical Society, 162, F327-F339.

[28] Skrzypkiewicz M., Lubarska-Radziejewska I., Jewlski J. (2015). The effect of Fe_2O_3 catalyst on direct carbon fuel cell performance. *International Journal of Hydrogen Energy*, 40, 13090-13098.

[29] Cai W., Liu J., Yu F., Zhou Q., Zhang Y., Wang X., Liu M., Ni M. (2017). A high performance direct carbon solid oxide fuel cell fueled by Ca-loaded activated carbon. *International Journal of Hydrogen Energy*, 42, 21167-21176.

[30] Li, X., Zhu, Z., De Marco, R., Bradley, J., Dicks, A. (2010). Modification of coal as a fuel for the direct carbon fuel cell. Journal of Physical Chemistry A, 114(11), 3855-3862.

[31] Vu, D.-L., Lee, C.G. (2016). Oxidation of ash-free coal from sub-bituminous and bituminous coals in a direct carbon fuel cell. Korean Journal of Chemical Engineering, 33(2), 507-513.

[32] Fuente-Cuesta, A., Jiang, C., Arenillas, A., Irvine, J.T.S. (2016). Role of coal characteristics in the electrochemical behaviour of hybrid direct carbon fuel cells. Energy and Environmental Science, 9(9), 2868-2880.

[33] Dudek, M., Skrzypkiewicz, M., Moskała, N., Grzywacz, P., Sitarz, M., Lubarska-Radziejewska, I. (2016). The impact of physicochemical properties of coal on direct carbon solid oxide fuel cells. International Journal of Hydrogen Energy, 41(41), 18872-18883.

[34] Ju, H.K., Eom, J., Lee, J.K., Choi, H.-K., Lee, S.-H., Song, R.-H., Lee, J. (2012). The activity of ash-free coal in direct carbon fuel cells. ECS Transactions, 50(49), 71-79.

[35] Kaklidis, N., Garagounis, I., Kyriakou, V., Besikiotis, V., Arenillas, A., Menendez, J.A., Marnellos, G.E., Konsolakis, M. (2015). Direct utilization of lignite coal in a Co-CeO_2/YSZ/Ag solid oxide fuel cell. *International journal of hydrogen energy*, 40(41), 14353–14363.

[36] Ali, A., Shehzad Bashir, F., Raza, R., Rafique, A., Kaleem Ullah, M., Alvi, F., Afzal, M., Ghauri, M., Belova, L.M. (2018). Electrochemical study of composite materials for coal-based direct carbon fuel cell. *International Journal of Hydrogen En*ergy, 43(28), 12900-12908.

[37] Deleebeeck, L., Gil, V., Ippolito, D., Campana, R., Kammer Hansen, K., Holtappels, P. (2017). Direct coal oxidation in modified solid oxide fuel cells. *Journal of the Electrochemical Society*, 164(4), F333-F337.

[38] Jiang, C., Ma, J., Arenillas, A., Bonaccorso, A.D., Irvine, J.T.S. (2016). Comparative study of durability of hybrid direct carbon fuel cells with anthracite coal and bituminous coal. *International Journal of Hydrogen Energy*, 41(41), 18797-18806

[39] Liu, G., Zhou, A., Qiu, J., Zhang, Y., Cai, J., Dang, Y. (2016). Utilization of bituminous coal in a direct carbon fuel cell. *International Journal of Hydrogen Energy*, 41(20), 8576-8582.

[40] Yue, X., Arenillas, A., Irvine, J.T.S. (2016). Application of infiltrated LSCM-GDC oxide anode in direct carbon/coal fuel cells. *Faraday Discussions*, 190, 269-289

[41] Deleebeeck, L., Arenillas, A., Menéndez, J.A., Kammer Hansen, K. (2015). Hybrid direct carbon fuel cell anode processes investigated using a 3-electrode half-cell setup. *International Journal of Hydrogen Energy*, 40(4), 1945-1958.

[42] Jiang, C., Ma, J., Arenillas, A., Irvine, J.T.S. (2013). Hybrid direct carbon fuel cells with different types of mineral coal. *ECS Transactions*, 57(1), 3013-3021.

[43] Kaklidis, N., Kyriakou, V., Marnellos, G.E., Strandbakke, R., Arenillas, A., Menéndez, J.A., Konsolakis, M. (2016). Effect of fuel thermal pretreatment on the electrochemical performance of a direct lignite coal fuel cell. *Solid State Ionics*, 288, 140-146.

[44] Zhu Y., Zhou W., Ran R., Chen Y., Shao Z., Liu M. (2016). Promotion of Oxygen Reduction by Exsolved Silver Nanoparticles on a Perovskite Scaffold for Low-Temperature Solid Oxide Fuel Cells. *Nano Lett.*, 16, 512-518.

[45] Sakito Y., Hirano A., Imanishi N., Takeda Y., Yamamoto O., Liu Y. (2008). Silver infiltrated $La_{0.6}Sr_{0.4}Co_{0.2}Fe_{0.8}O_3$ cathodes for intermediate temperature solid oxide fuel cells. *Journal of Power Sources*, 182, 476-481.

[46] Sun C., Hui R., Roller J. (2009). Cathode materials for solid oxide fuel cells: a review. *Journal of Solid State Electrochemistry*, 14, 1125-1144.

[47] Zhang J., Ji Y., Gao H., He T., Liu J. (2005). Composite cathode $La_{0.6}Sr_{0.4}Co_{0.2}Fe_{0.8}O_3$ - $Sm_{0.1}Ce_{0.9}O_{1.95}$–Ag for intermediate-temperature solid oxide fuel cells. *J. All. Comp.*, 395, 322-325.

[48] Chen, M., Wang, c., Niu, X., Zhao, S., Tang, J., Zhu, B. (2010). Carbon anode in direct carbon fuel cell. *International Journal of Hydrogen Energy*, 35, 2732-2736.

[49] Bonaccorso A.D., Jiang C., Ma J., Irvine J.T.S. (2016). Studies of current collection configurations and sealing for tubular hybrid-DCFC. *International Journal of Hydrogen Energy*, 41(41), 18788-18796.

[50] Gil V., Gurauskis J., Deleebeeck L., Stamate E., Kammer Hansen K. (2017). Cathode-supported hybrid direct carbon fuel cells. *International Journal of Hydrogen Energy*, 42, 4311-4319.